

# Journal of Materials Chemistry A

Accepted Manuscript



This is an *Accepted Manuscript*, which has been through the Royal Society of Chemistry peer review process and has been accepted for publication.

*Accepted Manuscripts* are published online shortly after acceptance, before technical editing, formatting and proof reading. Using this free service, authors can make their results available to the community, in citable form, before we publish the edited article. We will replace this *Accepted Manuscript* with the edited and formatted *Advance Article* as soon as it is available.

You can find more information about *Accepted Manuscripts* in the [Information for Authors](#).

Please note that technical editing may introduce minor changes to the text and/or graphics, which may alter content. The journal's standard [Terms & Conditions](#) and the [Ethical guidelines](#) still apply. In no event shall the Royal Society of Chemistry be held responsible for any errors or omissions in this *Accepted Manuscript* or any consequences arising from the use of any information it contains.

## Photonic crystal coupled porous BiVO<sub>4</sub> hybrid for efficient photocatalysis under visible light irradiation

Tianyu Huo, Xiufang Zhang\*, Xiaoli Dong, Xinxin Zhang, Chun Ma, Guowen Wang, Hongchao Ma, Mang Xue

School of Light Industry and Chemical Engineering, Dalian Polytechnic University, Dalian, China, 116034

\* Corresponding authors. Tel.: +86 411 86323508; fax: +86 411 86323736. E-mail address:

[zhangxf@dlpu.edu.cn](mailto:zhangxf@dlpu.edu.cn).

### Abstract

A bilayer TiO<sub>2</sub> photonic crystal (PC)/porous BiVO<sub>4</sub> was constructed by using liquid-phase deposition (LPD) and spin coating method for the enhancement of visible-light-driven photocatalytic ability through intensifying the light absorbance. The crystal form, morphology and film thickness, and light absorption performance were investigated. The photocatalytic activity of the bilayer TiO<sub>2</sub> PC/ porous BiVO<sub>4</sub> film was evaluated by the degradation of MB and was compared with that of porous BiVO<sub>4</sub> film. And the effect of the film thickness of the porous BiVO<sub>4</sub> on its photocatalytic ability was determined. It was found that the film thickness significantly affected the light absorption, and then, its photocatalytic ability, and the bilayer film with 1.03 μm of thickness of porous BiVO<sub>4</sub> film exhibited the highest photocatalytic performance. The photocatalytic ability of porous BiVO<sub>4</sub> was enhanced by combination the TiO<sub>2</sub> PC layer as the back reflector. This increase could be attributed to the intensified light absorbance produced by the reflect action from the TiO<sub>2</sub> PC. The effects of construction of porous structure and the application of photoelectrocatalytic process on the photocatalytic performance were also discussed.

## 1. Introduction

Photocatalytic pollutant degradation using semiconductor materials has attracted considerable attention due to the potential for the pollution control utilizing solar light.<sup>1-7</sup> The development of an efficient visible-light-driven semiconductor material is indispensable for the practical application. Monoclinic scheelite crystal  $\text{BiVO}_4$ , with a narrow band gap of 2.4 eV, has been certified to have photocatalytic ability for pollutant elimination.<sup>8,9</sup> Some efforts have been pursued to enhance its photocatalytic performance, such as noble metal modification,<sup>10, 11</sup> and heterojunction composite fabrication.<sup>12, 13</sup> Despite all the advances in the modifications,  $\text{BiVO}_4$  still suffers from limited light absorption, which partly accounts for its poor photoactivity.

Photonic crystal (PC) is periodic optical material or structure that is designed to confine, control and manipulate photons so as to intensify the light absorption, and enhance the related performance of the material.<sup>14-17</sup> The periodic modulation of PC leads to a photonic band gap, the light in the wavelength range of which cannot propagate in the PC due to the Bragg diffraction and scattering on lattice planes generally named as band gap scattering effect,<sup>18, 19</sup> but can be reflected by the PC. Thus, the PC acts as a dielectric mirror to reflect the light in the wavelength range of photonic band gap. Because of the property, PC can be used to enhance the light absorption of photoresponsive material by multiple scattering. For example, Yu et al.<sup>20</sup> reported that the power conversion efficiency of polymer solar cells was enhanced with the PC as a high reflector. Liao et al.<sup>21</sup> found that using inverse  $\text{TiO}_2$  opal PC as a mirror could promote the light absorption so as to enhance the photocatalytic

capability of the photocatalyst. The film thickness of the photoresponsive material (photocatalyst) is particularly vital. Light intensity usually attenuates as it penetrates into the solid photocatalyst film.<sup>22, 23</sup> If the film thickness is larger than the light penetration depth, the light will not illuminate on the PC, the PC will not promote the absorption of the photocatalyst.

Another solution to enhance the absorption is to fabricate the photocatalyst with porous structure.<sup>24-26</sup> The light absorption is intensified by the channels serving as light-transfer paths for the distribution of photon energy onto the large surface of inner photocatalyst particles. Otherwise, photoelectrocatalysis is a promising technique to improve the efficiency of photocatalytic process.<sup>27, 28</sup> The photogenerated electron can be drawn from work electrode to the counter electrode by the bias potential and the separation efficiency of photogenerated electron-hole pairs can be elevated.

Herein, we constructed an inverse TiO<sub>2</sub> opal PC coupled porous BiVO<sub>4</sub> film (bilayer TiO<sub>2</sub> PC/porous BiVO<sub>4</sub> film) on FTO substrate for efficient visible-light-driven photocatalysis. The inverse TiO<sub>2</sub> opal PC, a common kind of PC, was used as the back reflector to enhance the absorbance, and ultimately elevate the photocatalytic ability of BiVO<sub>4</sub> film. The effect of the thickness of BiVO<sub>4</sub> on the photocatalytic ability was firstly discussed. MB was chosen as a probe to test photocatalytic activities of the prepared samples.

## 2. Experimental section

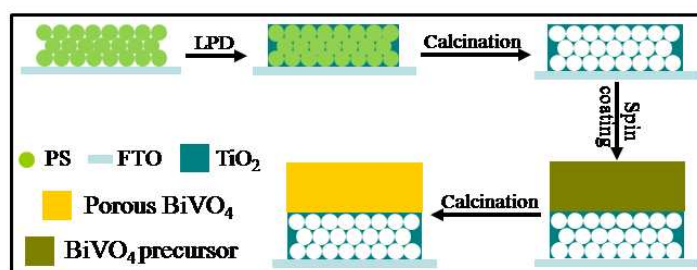
**Materials.** Monodisperse polystyrene latex sphere suspension (193 nm, 2 wt % in water) was purchased as the template from Shenzhen Nano-Micro Technology Co.,

Ltd. Vanadium (V) tri-*i*-propoxy oxide was purchased as the vanadium source from Strem Chemicals, USA. Bismuth ( $\square$ ) nitrate pentahydrate was purchased as the bismuth source from Tianjin Kermel Chemical Reagents Development Centre, China. FTO glass with a thickness of 2.2 mm and a sheet resistance of 15  $\Omega$ /square from Geao Co., Chian, was used as the substrate. All the reagents were used without further purification.

**Preparation of TiO<sub>2</sub> PC.** TiO<sub>2</sub> PC was prepared by the method reported by Lu et al.<sup>29</sup> In detail, FTO substrates were cleaned in ultrasonic bath with dilute HCl and ethanol, respectively, and then rinsed with deionized water and dried in air. The colloidal crystal polystyrene film was prepared via solvent evaporation method. The suspension of polystyrene spheres was diluted with deionized water to a concentration of 0.1 wt%, and then was sonicated in a glass vial for 30 min to brake aggregation. FTO substrates were immersed vertically in the suspension in the glass vial. The polystyrene spheres were aligned on the FTO (named as polystyrene opals) by keeping the glass vial in an oven at 55 °C overnight to fully evaporate the water in the suspension. To fabricate the inverse TiO<sub>2</sub> opal, the reported liquid-phase deposition (LPD) method was used to replicate the polystyrene opal. The polystyrene opal film was immersed vertically in a solution of 0.15 wt % titanium isopropoxide and 0.015% HNO<sub>3</sub> in ethanol for 5 min to form a TiO<sub>2</sub> seed layer. After dried in air, it was dipped in an aqueous solution of 0.1 M ammonium hexafluorotitanate and 0.3 M boric acid at 60 °C. The pH of the solution was adjusted to about 3 by adding 1 M hydrochloric acid. After 25 min, the samples were washed thoroughly with deionized water and

dried in air. The polystyrene spheres were removed by calcining the film at 500 °C for 2 h with a heating rate of 2 °C/min, and then, the inverse TiO<sub>2</sub> opal PC was obtained.

**Preparation of bilayer TiO<sub>2</sub> PC/porous BiVO<sub>4</sub> film.** The BiVO<sub>4</sub> precursor was prepared by mixing solution A (obtained by dissolving bismuth nitrate in acetic acid) and B (obtained by dissolving vanadium (V) tri-isopropoxy oxide in acetylacetone) with a 1:1 stoichiometric ratio of Bi to V. The sol was vigorously stirred for 0.5 h, and the prepared polystyrene spheres were added in the sol as the template to form the pores. The bilayer TiO<sub>2</sub> PC/porous BiVO<sub>4</sub> films were obtained by depositing the above sol on the FTO glass by a spin coater and annealed in air at 500 °C for 2 h. The coating and annealing processes were repeated to result in different coating layers, and the films were recorded by S<sub>n</sub>, where n was the number of the layer of the film. The schematic procedure for preparing bilayer TiO<sub>2</sub> PC/porous BiVO<sub>4</sub> film was presented in Scheme 1. Porous BiVO<sub>4</sub> film and BiVO<sub>4</sub> film were prepared by the same process but directly on the FTO, and the number of the layer was four. The precursor of BiVO<sub>4</sub> film was the same as the porous BiVO<sub>4</sub> film without the template.



Scheme 1. Schematic procedure for preparing bilayer TiO<sub>2</sub> PC/porous BiVO<sub>4</sub> film.

**Characterization.** The crystal structure of the films was characterized by Rigaku D/MAX2400 with Cu K $\alpha$  radiation, current of 30 mA, accelerating voltage of 40 kV

and a scanning rate of 0.02°/s in the  $2\theta$  range of 10-80°. The scanning electron microscopy images of the films were investigated by a Hitachi S-4800 with an accelerating voltage of 30.0 kV. UV-visible transmittance spectra of the samples were recorded on a UV-vis spectrophotometer (Shimadzu, UV-2450) with a wavelength range of 200-800 nm.

**Photoelectrocatalytic degradation of MB.** The photoelectrocatalytic degradation of MB was performed in a cubic quartz reactor. The initial concentration and volume of MB were 5 mg/L and 75 mL, respectively, and 0.01M sodium sulfate was used as the electrolyte. The prepared film electrode, a platinum foil and a SCE served as photo-anode, cathode and the reference electrode, respectively. The bias potential (0.8 V vs. SCE) was applied using a CHI electrochemical analyzer (CHI 660D, Shanghai Chenhua, China). A 300 W Xe lamp (PLS-SXE 300, Beijing Bofeilai Science and Technology Co., China) served as the visible light source. The light was passed through a glass filter, which only permitted the light with wavelength above 400 nm to illuminate on the photo-anode electrode. Photocatalytic and electrochemical experiment were done under the same condition without the bias potential and illumination, respectively. The adsorption experiment was performed without the bias potential and illumination. And direct photolysis experiment was done under the illumination of light same as the photoelectrocatalytic process. The concentration of MB was determined by UV-vis spectrophotometer (UV-721, Xinmao) at 664 nm.

### 3. Results and Discussion

**Crystal form.** The XRD patterns are shown in Fig. 1. The crystal form of BiVO<sub>4</sub> can be identified to be monoclinic scheelite type according to the observed

characteristic peaks with  $2\theta$  at  $18.8^\circ$ ,  $28.8^\circ$ ,  $30.5^\circ$ ,  $39.7^\circ$  and  $53.1^\circ$  (JCPDS No.14-0688), which has the most excellent photocatalytic ability among its three crystal forms (tetragonal zircon type, tetragonal scheelite type and monoclinic scheelite type). Besides, other peaks ( $26.5^\circ$ ,  $38.2^\circ$  and  $52.0^\circ$ ) in the patterns of bilayer  $\text{TiO}_2$  PC/porous  $\text{BiVO}_4$  film, porous  $\text{BiVO}_4$  film and  $\text{BiVO}_4$  film are found, which are the peaks of FTO. The peaks of  $\text{TiO}_2$  are not clear even in the pattern of  $\text{TiO}_2$  PC film, which may be hidden by the spectral peak of FTO ( $25.3^\circ$  of  $2\theta$  of the main peak of anatase  $\text{TiO}_2$ ) or/and be attributed to the less amount of  $\text{TiO}_2$ .

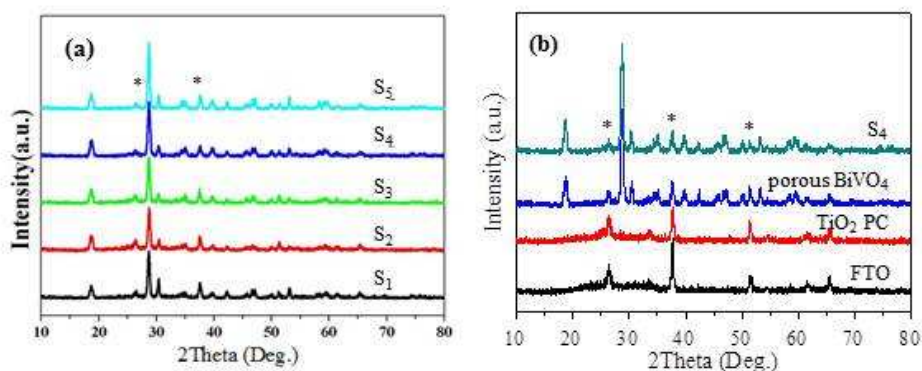


Fig.1 XRD patterns of (a)  $S_1$ ,  $S_2$ ,  $S_3$ ,  $S_4$  and  $S_5$ , (b) FTO,  $\text{TiO}_2$  PC film, porous  $\text{BiVO}_4$  film and bilayer  $\text{TiO}_2$  PC/porous  $\text{BiVO}_4$  film ( $S_4$ ). (\*) FTO peaks.

**Morphology and film thickness.** Fig. 2 shows SEM images of  $\text{TiO}_2$  PC and  $S_4$ . It can be observed that the perfect periodic structure in the  $\text{TiO}_2$  PC (Fig. 2 (a)) has been obtained. The average diameter of the hollow spheres is around 193 nm, which is similar to the size of the template, inferring that it is the replica of the polystyrene sphere. The perfect  $\text{TiO}_2$  PC will modulate the light efficiently, and will be an excellent back reflector for the upper layer of the photocatalyst. Porous structure of  $\text{BiVO}_4$  layer is confirmed by the SEM image of top view of  $S_4$ . Fig. 2 (c) displays the

cross section image of  $S_4$ .  $S_4$  is constructed with FTO,  $\text{TiO}_2$  PC layer, and the porous  $\text{BiVO}_4$  layer. The thickness of the  $\text{TiO}_2$  PC layer and porous  $\text{BiVO}_4$  layer are about 0.8 and 1.0  $\mu\text{m}$ , respectively. The thickness of the bilayer films is further detected, and the result is illustrated in Fig. 2 (d). The film thickness increases from 0.72 ( $S_1$ ) to 1.90  $\mu\text{m}$  ( $S_5$ ), indicating repeating the coating process can indeed increase the thickness of the film. Furthermore, the thickness of  $S_4$  is 1.63  $\mu\text{m}$ , which is similar to the result obtained by SEM.

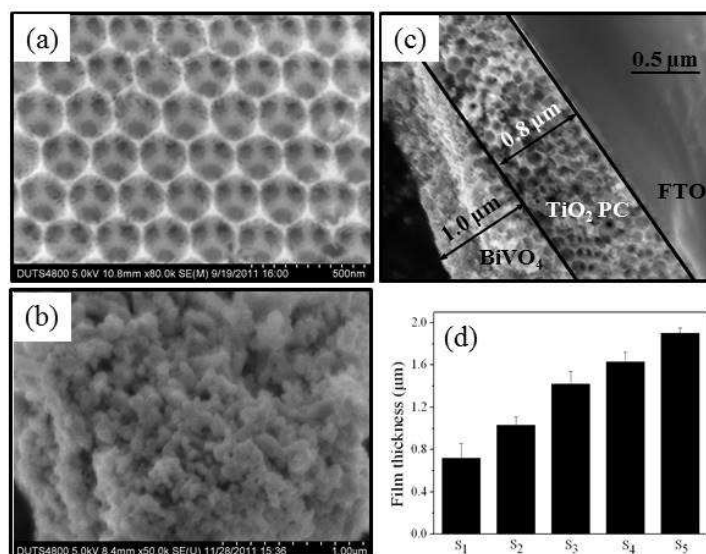


Fig. 2 SEM images of top view of (a)  $\text{TiO}_2$  PC, (b) top view of  $S_4$ , (c) cross section view of  $S_4$  and (d) the film thickness of  $S_1$ ,  $S_2$ ,  $S_3$ ,  $S_4$  and  $S_5$ .

**Light absorption ability.** It is well known that the optical absorption ability is the key factor in determining the photocatalytic ability. More photos are absorbed, more electron and hole pairs will be generated, and more efficient photocatalytic ability will be obtained. UV-vis diffuse reflectance spectra are displayed in Fig. 3. From Fig. 3 (a), the transmittance of the bilayer films decreases with the layer of the film increasing

from one to four. However, the transmittance of  $S_5$  rises. This law is obvious in the wavelength range from 400 to 520 nm (inset of Fig. 3 (a)), the light in which can excite the  $\text{BiVO}_4$ . The film thickness of  $S_5$  may be larger than the light penetration depth, and the  $\text{TiO}_2$  PC is out of function, which make the decrease of the absorbance of  $S_5$ . From Fig. 3 (b), the transmittance of FTO is big in the wavelength range of 400-800 nm, because it is transparent.  $\text{TiO}_2$  PC has an obvious band gap, and its center, blue edge and red edge of the band gap are at 450, 400 and 550 nm, respectively. Compared with  $\text{BiVO}_4$  film, the porous  $\text{BiVO}_4$  film has lower transmittance, which can be attributed to the distribution action of light photos by the pores. Furthermore, the transmittance of  $S_4$  is smaller than that of porous  $\text{BiVO}_4$  film especially between the center and the red edge of the band gap. The intensified absorbance can be attributed to the scattering effect generated by the  $\text{TiO}_2$  PC. As the back reflector,  $\text{TiO}_2$  PC can reflect the light in the band gap. Thus, the light can “illuminate”  $\text{BiVO}_4$  film again, and then, the absorbance is enhanced. Based on the result got by the analysis of UV-vis diffuse reflectance spectra, it is reasonably predicted that  $S_4$  has excellent photocatalytic performance.

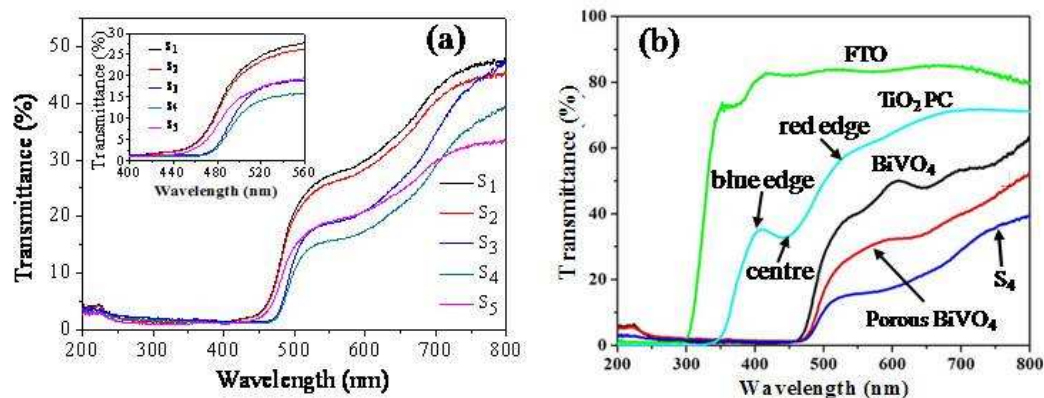


Fig. 3 UV-vis diffuse reflectance spectra of (a)  $S_1$ ,  $S_2$ ,  $S_3$ ,  $S_4$  and  $S_5$ , inset is magnified spectra

(wavelength from 400 to 560 nm) of (a), and (b) FTO, TiO<sub>2</sub> PC film, BiVO<sub>4</sub> film, porous BiVO<sub>4</sub> film and S<sub>4</sub>.

**Photocatalytic performance.** MB is chosen as the model substance to test the photocatalytic ability of the as prepared samples, and the result is illustrated in Fig. 4. From Fig. 4 (a), the removal rate of MB in the photoelectrocatalytic process increases S<sub>1</sub> to S<sub>4</sub>, this enhancement can be attributed to their elevated absorption ability. However, the photoelectrocatalytic ability of S<sub>5</sub> decreases. The reason for this decrease is its fall of absorption ability. Furthermore, the photoelectrocatalytic degradation rate is also affected by the transport of reactants to and from the bulk solution. The reactants have a longer diffusion path to the interior BiVO<sub>4</sub> due to the thicker film of S<sub>5</sub>,<sup>30</sup> and thus, the decreased removal rate of S<sub>5</sub> is got. In 180 min, the MB removal efficiency is 8.12% with S<sub>4</sub> in electrochemical process Fig. 4 (b), but it is 6.88% in the adsorption process, the comparison result shows that the electrochemical process can be neglected. The MB removal rate is 19.6% in the direct photolysis, indicating that MB can be slightly decomposed under the illumination of visible light. Porous BiVO<sub>4</sub> has excellent photocatalytic ability regarding 80.1% of elimination rate of MB in photocatalytic process, though adsorption process and/or direct photolysis contributes a small part to the whole elimination rate. Based on 91.6% of the removal rate in the photoelectrocatalytic process, the photocatalytic ability of S<sub>4</sub> is enhanced by the potential bias, which can efficiently separate the photogenerated electron-hole pairs by transporting the photogenerated electron to the counter electrode, and therefore increase the photocatalytic ability. The photocatalytic performance of BiVO<sub>4</sub> film, porous BiVO<sub>4</sub> film and bilayer TiO<sub>2</sub> PC/porous BiVO<sub>4</sub> film (S<sub>4</sub>) in

photoelectrocatalytic process is compared (Fig. 3 (c)). In 180 min, only 57.8% of MB is removed with BiVO<sub>4</sub> film, however, MB removal rate with porous BiVO<sub>4</sub> film is 63.5%, indicating mesoporous structure produced can enhance the photocatalytic performance of BiVO<sub>4</sub>. The photocatalytic ability is further elevated by adding the TiO<sub>2</sub> PC film as the back layer (91.6%). It is found that the MB elimination in four processes followed the pseudo-first-order kinetics by the linear transforms  $\ln(C_0/C_t) = -kt$  ( $k$  is kinetic constant). The  $k$  of MB removal in photoelectrocatalytic process with S<sub>4</sub> (0.0138 min<sup>-1</sup>) is 2.38 times that with porous BiVO<sub>4</sub> film (0.00579 min<sup>-1</sup>), and is 2.83 times (0.00487 min<sup>-1</sup>). This enhancement can be attributed to the mesoporous structure and the reflect action of PC, which elevate the absorption ability. Bilayer TiO<sub>2</sub> PC/porous BiVO<sub>4</sub> with high absorbance can be excited by more photos, and more electrons and holes can be photo-generated. Then an increased number of electrons and holes participates the oxidation of MB. Therefore, the enhanced MB elimination rate is obtained.

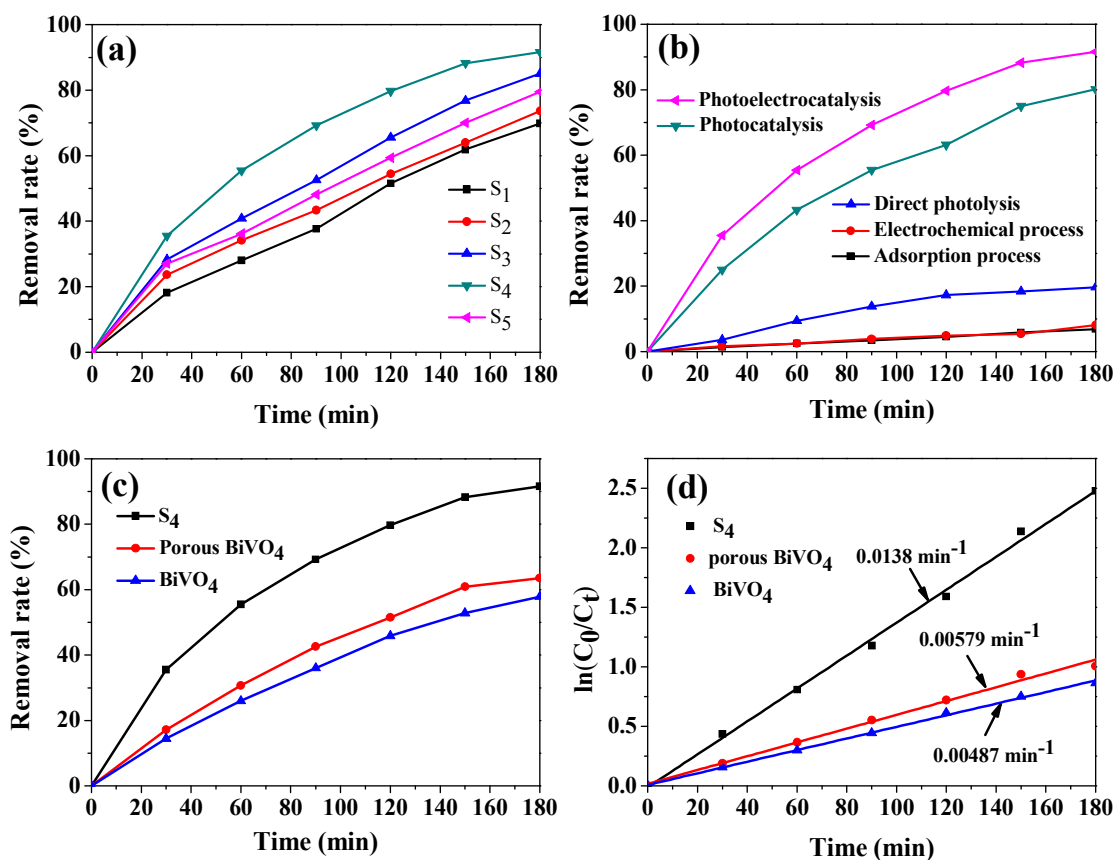


Fig. 4 MB degradation rate vs reaction time plotted for (a) photoelectrocatalytic degradation with S<sub>1</sub>, S<sub>2</sub>, S<sub>3</sub>, S<sub>4</sub> and S<sub>5</sub>, (b) degradation in various processes with S<sub>4</sub>, (c) photoelectrocatalytic degradation with S<sub>4</sub>, porous BiVO<sub>4</sub> film and BiVO<sub>4</sub> film and (d) ln(C<sub>0</sub>/C<sub>t</sub>) vs reaction time in photoelectrocatalytic process with S<sub>4</sub>, porous BiVO<sub>4</sub> film and BiVO<sub>4</sub> film under visible light.

#### 4. Conclusions

Bilayer TiO<sub>2</sub> PC/porous BiVO<sub>4</sub> has been successfully constructed. The thickness of porous BiVO<sub>4</sub> film significantly affects the absorption ability. The absorbance of BiVO<sub>4</sub> film is enhanced by the reflect action of light of TiO<sub>2</sub> PC combined with the distribution action of photos of porous structure. The photocatalytic ability of BiVO<sub>4</sub> film is enhanced by the construction of porous structure and bilayer film with TiO<sub>2</sub> PC. This enhancement can be attributed to the increase of absorption ability. Bilayer TiO<sub>2</sub> PC/porous BiVO<sub>4</sub> with high absorbance can be excited by more photos, more

electrons and holes can subsequently be photo-generated, at last, an increased number of electrons and holes participate the oxidation of model substance. Based on the results got here, it is confirmed that the configuration of the visible-light-driven photocatalyst in this work can be significant in the field of photocatalytic process to meet the requirements of environmental pollution control in future.

### Acknowledgement

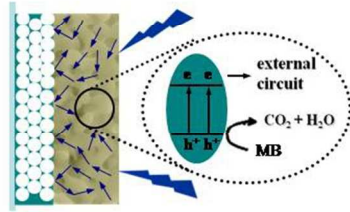
This work was supported by the National Science Fund China (project No. 21107007) and Cultivation Program for Excellent Talents of Science and Technology Department of Liaoning Province (No. 2014026009).

### References

- [1] L. F. Yin, J. F. Niu, Z. Y. She and J. Chen, *Environ. Sci. Technol.*, 2010, **44**, 5581-5586.
- [2] M. Y. Wang, L. Sun, Z. Q. Lin, J. H. Cai, K. P. Xie and C. J. Lin, *Energy Environ. Sci.*, 2013, **6**, 1754-5692
- [3] M. Y. Wang, J. Loccozia, L. Sun, C. J. Lin and Z. Q. Lin, *Energy Environ. Sci.*, 2014, **7**, 2182-2202.
- [4] M. D. Ye, D. J. Zheng, M. Y. Wang, C. Chen, W. M. Liao, C. J. Lin and Z. Q. Lin, *ACS Appl. Mater. Interfaces*, 2014, **6**, 2893-2901.
- [5] X. D. Zhang, W. M. Liao, W. Wu, D. J. Zheng, Y. S. Zhou, B. L. Xue, W. Liu, Z. Q. Lin and Y. L. Deng, *J. Mater. Chem. A*, 2014, **2**, 11035-11039.
- [6] N. Kajiwara, Y. Noma and H. Takigami, *Environ. Sci. Technol.*, 2008, **42**, 4404-4409.
- [7] M. D. Ye, M. Y. Wang, D. J. Zheng, N. Zhang, C. J. Lin and Z. Q. Lin, *Nanoscale*, 2014, **6**, 3576-3584.
- [8] A. Kudo, K. Omori and H. Kato, *J. Am. Chem. Soc.*, 1999, **121**, 11459-11467.

- [9] S. Tokunaga, H. Kato and A. Kudo, *Chem. Mater.*, 2001, **13**, 4624-4628.
- [10] S. Kohtani, J. Hiro, N. Yamamoto, A. Kudo, K. Tokumura and R. Nakagaki, *Catal. Commun.*, 2005, **6**, 185-189.
- [11] A. P. Zhang and J. Z. Zhang, *J. Alloys. Compd.* 2010, **491**, 631-635.
- [12] S. Ho-Kimura, S. J. A. Moniz, A. D. Handoko and J. W. Tang, *J. Mater. Chem. A*, 2014, **2**, 3948-3953.
- [13] H. Q. Jiang, H. Endo, H. Natori, M. Nagai and K. Kobayashi, *Mater. Res. Bull.*, 2009, **44**, 700-706.
- [14] J. L. Chen, E. Loso, N. Ebrahim and G. A. Ozin, *J. Am. Chem. Soc.*, 2008, **130**, 5420-5421.
- [15] S. Guldin, S. Huttner, M. Kolle, M. E. Welland, P. Muller-Buschbaun, R. H. Friend, U. Steiner and N. Tetreault, *Nano Lett.*, 2010, **10**, 2303-2309.
- [16] X. Q. Chen, J. H. Ye, S. X. Ouyang, T. Kako, Z. S. Li and Z. G. Zou, *ACS Nano.*, 2011, **5**, 4310-4318.
- [1] J. Liu, M. Z. Li, J. X. Wang, Y. L. Song and L. Jiang, *Environ. Sci. Technol.*, 2009, **43**, 9425-9431.
- [18] P. L. Flaugh, S. E. O' Donnell and S. A. Asher, *Appl. Spectrosc.*, 1984, **38**, 847-850.
- [19] R. J. Carlson and S. A. Asher, *Appl. Spectrosc.*, 1984, **38**, 297-304.
- [20] W. J. Yu, L. Shen, P. Shen, Y. B. Long, H. W. Sun, W. Y. Chen and S. P. Ruan, *ACS Appl. Mater. Inter.*, 2014, **6**, 599-605.
- [21] G. Z. Liao, S. Chen, X. Quan, H. Chen and Y. B. Zhang, *Environ. Sci. Technol.*, 2010, **44**, 3481-3485.
- [22] H. T. Chang, N. Wu and F. Zhu, *Water Res.*, 2000, **34**, 407-416.

- [23] X. C. Wang, J. C. Yu, C. Ho, Y. D. Hou and X. Z. Fu, *Langmuir*, 2005, **21**, 2552-2559.
- [24] J. G. Yu, L. J. Zhang, B. Cheng, Y. R. J. Su, *J. Phys. Chem. C*, 2007, **111**, 10582-10589.
- [25] L. W. Zhang, Y. J. Wang, H. Y. Cheng, W. Q. Yao, Y. F. Zhu, *Adv. Mater.*, 2009, **21**, 1286-1290.
- [26] W. Y. Gan, H. J. Zhao and R. Amal, *Appl. Catal. A*, 2009, **354**, 8-16.
- [27] X. Z. Li, H. L. Liu and P. T. Yue, *Environ. Sci. Technol.*, 2000, **34**, 4401-4406.
- [28] X. F. Zhang, S. Chen, X. Quan and H. M. Zhao. *Sep. Purif. Technol.*, 2009, **64**, 309-313.
- [29] Y. Lu, H. T. Yu, S. Chen, X. Quan, and H. M. Zhao, *Environ. Sci. Technol.*, 2012, **46**, 1724-1730.
- [30] H. F. Zhuang, C. J. Lin, Y. K. Lai, L. Sun and J. Li, *Environ. Sci. Technol.*, 2007, **41**, 4735-4740.



254x190mm (96 x 96 DPI)